Effects of Nitrogen on the Activation/Deactivation of Boron and Indium in N-channel CMOS Devices

Sheldon Aronowitz, Helmut Puchner, and Vladimir Zubkov
LSI Logic Corporation
3115 Alfred Street
Santa Clara, CA 95054, USA
email: sheldon@lsil.com

***Abstract*—Activation/deactivation behavior of combinations of electrically active dopants boron and indium with nitrogen was studied both experimentally and quantum chemically. It was found that direct correlations could be made between relative electrical activity and top-filled / lowest-empty molecular orbitals obtained with a model silicon lattice system. The trend in activation explained the device behavior observed when retrograde indium channels in NMOS devices were created with nitrogen present to control gate oxide growth.**

I. Introduction

Retrograde 0.18 mm channel devices were successfully created using indium threshold voltage implants. Because of dual oxide requirements nitrogen was co-implanted into the channel region to control gate oxide growth resulting in a decrease of the threshold voltage to an unacceptable level. To explain this unexpected behavior a thorough study then was undertaken to determine experimentally and theoretically whether the observed deactivation of the channel dopants could be quantified, explained and altered. As there are no suitable activation/deactivation models for this specific combination of dopants available we successfully employed a quantum chemical code to investigate the electrical activity of different dopant combinations.

The unanticipated device behavior when pre-gate nitrogen was introduced into retrograde channels created with indium was unambiguous in detail and dramatic in magnitude.

II. Pre-gate Nitrogen Implant Effect on an Indium N-channel Device

Super-steep retrograde n-channel devices were created using indium implants. The experimental threshold voltage behavior formed with an indium-only channel over a range of gate lengths is displayed in Figure 1 by the curve with filled diamond markers. The gate oxide thickness was $3.5nm$. The channel was formed using a $7 \cdot 10^{12} In^{+}/cm^{2}@190keV$ implant. The pocket implant dose was $5 \cdot 10^{12} P^{+}/cm^{2}$. The second curve, with the open circles, in Figure1 presents the effect of a $2 \cdot 10^{14} N2^{+}/cm^{2}$ pre-gate nitrogen implant on a NMOS device. There were slight differences in processing from the first device: the indium dose was slightly reduced to $6.5 \cdot 10^{12} In^{+}/cm^{2}$, the pocket implant dose was changed to $4 \cdot 10^{12} P^{+}/cm^{2}$ and the gate oxide thickness equaled $3.3nm$ rather than $3.5nm$. All other processing parameters were identical. The small change in the pocket implant dose has a negligible effect on the threshold voltage at long-channel lengths. The reduction in threshold voltage, slightly greater than $200mV$, can be attributed to three alternatives: (1) a large reduction in electrically active indium, (2) the nitrogen counter-doped the channel, or (3) a high density of interface states was created with nitrogen incorporation in the gate oxide. The counter-doping and interface state possibilities were eliminated with devices formed under the same conditions using boron. It was found that the threshold voltage was minimally reduced with channels formed with a boron implant and the same pre-gate nitrogen implant dose. The remaining highly probable inference then is that the nitrogen in some fashion interfered with the formation of electrically active indium. Without suitable models of electrical activation/deactivation of indium and boron in the presence of nitrogen, exploration using a quantum chemical approach became appealing.

III. Description of Self-consistent Charge Extended Huckel

The semiempirical quantum chemical method described in this section assumes that a hamiltonian operator $\mathbf{H}$ exists for any cluster of interacting atoms and that the eigenfunctions of this hamiltonian are the molecular orbitals ψ_j. Also assumed is that ψ_j can be represented by a linear combination of the i atomic orbitals, χ_{ki}, associated with the k atoms of the cluster where

$$\psi_j = \sum_{k,i} c_{jki} \cdot \chi_{ki} \tag{1}$$

The ψ_js are orthonormalized and their energies equal

$$\epsilon_j = \sum_{k,i} \sum_{v,u} c^{*}_{jki} \cdot c_{jvu} \cdot \int \chi^{*}_{ki} \cdot H \cdot \chi_{vu} d\tau. \tag{2}$$

Minimization of the energy with respect to the coefficients yields the secular determinant

0-7803-6279-9/00/$10.00 © 2000 IEEE

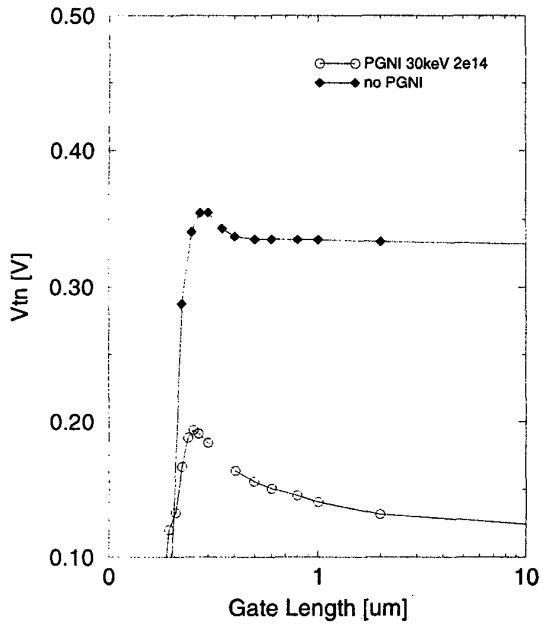

Fig. 1. Effect on the threshold voltage of super-steep retrograde n-channel devices created with indium when a pre-gate nitrogen implant (PGNI) is either absent or present.

$$\begin{aligned} \left|H_{i\{k\},u\{v\}} - \epsilon S_{i\{k\},u\{v\}}\right| &= 0, \\ H_{i\{k\},u\{v\}} &= \int \chi^*_{ki} \cdot H \cdot \chi_{vu} d\tau, \\ S_{i\{k\},u\{v\}} &= \int \chi^*_{ki} \cdot \chi_{vu} d\tau. \end{aligned} \quad (3)$$

$S_{i\{k\},u\{v\}}$ is the integrated overlap between the $i\{k\}$ and $u\{v\}$ orbitals. The atomic orbitals are represented by Slater-type functions,

$$\chi = C \cdot r^{n-1} \cdot exp(-\zeta_r) \cdot (angular function), \quad (4)$$

where C is a normalization constant, the *angular function* is a spherical harmonic, n is a principal atomic number and ζ, the orbital exponent, is optimized to ensure the energy minimum using a self-consistent field method [1,2]. Experimental data is incorporated in the prescription for the hamiltonian matrix elements. The diagonal element of the hamiltonian matrix associated with the i-th atomic orbital on the k-th atom for the $\ell+1$ iteration equals

$$H^{\ell+1}_{i\{k\},i\{k\}} = \left(1 - \left|Q^\ell_k\right|\right) \cdot \alpha^0_{i\{k\}} + \left|Q^\ell_k\right| \cdot \alpha^{\pm}_{i\{k\}} 0. \quad (5)$$

Q^ℓ_k is related to the calculated charge density q^ℓ_k in the following manner:

$$Q^\ell_k = \frac{(q^\ell_k + f \cdot Q^{\ell-1}_k)}{(1+f)} \quad (6)$$

The value of f is chosen to damp oscillations in large systems and permit convergence; assigning f a value of 10 usually suffices. $\alpha^0_{i\{k\}}$ and $\alpha^{\pm}_{i\{k\}}$ are the valence orbital ionization energies of the i-th orbital for the cases when the atom is either neutral or singly charged. These energies are empirically determined from spectroscopic data. The off-diagonal elements equal

$$H^{\ell+1}_{i\{k\},u\{v\}} = 0.5 \cdot K \left[H^{\ell+1}_{i\{k\},i\{k\}} + H^{\ell+1}_{u\{v\},u\{v\}}\right] S_{i\{k\},u\{v\}}. \quad (7)$$

K is a constant set equal to 1.89 in our calculations.

Inner atomic shells that are not explicitly treated reduce the effective core charge $Z_k\{core\}$ experienced by the valence electrons on the k-th atom. The charge density is related to the effective core charge and the electron density distributions associated with the occupied molecular orbitals. The calculations use the Mulliken approximation [3,4]. After the $\ell+1$ iteration, for example, the charge density on the k-th atom equals

$$\begin{aligned} q^{\ell+1}_k &= Z_k\{core\} - \sum_j \eta_j \sum_i \left[c^{\ell+1^*}_{jki} \cdot c^{\ell+1}_{jki} \right. \\ &\quad \left. + 0.5 \sum_{v,u} \delta_{i\{k\},u\{v\}} c^{\ell+1^*}_{jki} c^{\ell+1}_{jvu} S_{i\{k\},u\{v\}}\right], \\ \delta_{i\{k\},u\{v\}} &= 0, \quad i\{k\} = u\{v\}, \\ \delta_{i\{k\},u\{v\}} &= 1, \quad i\{k\} \neq u\{v\}. \end{aligned} \quad (8)$$

η_j is the occupation number for the j-th molecular orbital. Convergence is achieved when the largest absolute difference between the atomic charges of the ℓ-th and $\ell+1$ iterations is less than a pre-determined value.

The approach permits rapid examination of relatively large systems. The energies and eigenfunctions for a silicon+hydrogen cluster that has two hundred valence orbitals can be obtained in under five minutes on a Sun Ultra Sparc 2. All-neighbor interactions are included, there is no restriction with respect to planarity and charge redistribution effects can be determined.

IV. Quantum Chemical Results

The semi-empirical self-consistent charge extended Huckel method was used to explore the interactions of multiple species in the model cluster displayed in Figure 2. The approach has been successfully used in the past to delineate trends of dopant interactions in silicon [5] and in the crystalline layer of clays [6]. The model cluster contained 38 silicon atoms and dangling bonds were completed by hydrogen atoms. The final cluster was $Si_{38}H_{48}$. Several combinations of boron, indium and nitrogen were examined. The combinations of immediate interest involved boron and indium at substitutional sites and nitrogen at a hexagonal interstitial site when combined with the other dopant species. The results for the combinations of greatest interest are presented in Table I.

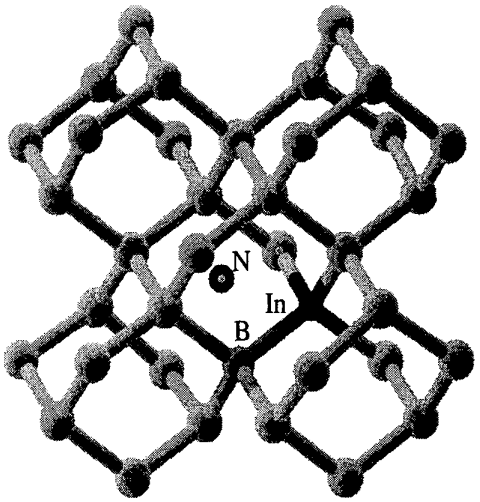

Fig. 2. Model silicon cluster with boron and indium at substitutional sites and nitrogen at an interstitial position (hydrogens completing silicon bonds are not shown).

The lowest vacant orbitals, the highest partially occupied orbitals and the highest fully occupied orbitals are displayed in Table I. Since boron or indium are acceptors, promotion of an electron from an occupied orbital to either a partially occupied orbital having boron or indium character or to the lowest vacant orbital that also possesses boron or indium character would correspond to the creation of a hole in the silicon crystal valence band. The relative electrical activity in the presence of nitrogen was predicted to decrease as the ΔE in Table I increases. The combination of boron, indium, and nitrogen should be the most inactive. Interactions between cluster dopants, as reflected in ΔE behavior, remained practically unchanged when distances between dopants were increased. Analysis of the self-consistent charge extended Huckel formalism showed that dopant interactions modify the eigenfunctions in a manner that effects are established over relatively long distances.

V. Comparison with Experimental Results

Experiments were performed involving the combinations of dopants examined in Table I. Indium ($1 \cdot 10^{13}\ In^{+}/cm^{2}$ @$180keV$), Nitrogen ($4 \cdot 10^{14}\ N^{+}/cm^{2}$@$40keV$), and Boron ($1 \cdot 10^{13}\ B^{+}/cm^{2}$@$25keV$) were implanted in different combinations into p-type wafers after $4.5nm$ of oxide was thermally grown. The energies of the implants were chosen to have their projected ranges coincide. These series of implants were used to create the combinations In, $In+B$, $In+N$, $In+B+N$, B, and $B+N$. The wafers were annealed under neutral ambient conditions at $1000°C$ for 30 seconds. SIMS and spreading resistance profiling (SRP) were performed on the various wafers. Table I lists the activation index from SRP with respect to the In and B combinations in the presence of nitrogen whereas Figure 3 displays the SRP results for all the combinations presented in Table I. The activation trend is in good qualitative agreement with the trend obtained from the self-consistent charge extended Huckel method.

TABLE I
Results of Quantum Chemical Calculations for B, In, B+N, In+N, B+In+N. Boron and Indium are at substitutional sites and nitrogen at an interstitial position in the model silicon cluster.

	Dopant Combinations					
	B	In	B+In	B+N	In+N	B+In+N
Orbital energy levels (in eV): lowest vacant or partially occupied / highest fully occupied	-5.50 ↑	-5.34 ↑	-5.46 –	-3.88 –	-3.23 –	-4.63 ↑
	-5.51 ↑↓	-5.37 ↑↓	-5.48 ↑↓	-4.02 ↑↓	-3.55 ↑↓	-5.64 ↑↓
	-5.81 ↑↓	-5.70 ↑↓	-5.83 ↑↓	-5.63 ↑↓	-5.30 ↑↓	-5.93 ↑↓
≈ ΔE (eV) for electron promotion	0.01	0.03	0.02	0.14	0.32	0.99
Activation index from SRP[a]	1	1	1	0.91	0.79	0.51

[a]The activation index is the ratio of the carrier dose when nitrogen is present to the carrier dose in absence of nitrogen.

The overlap population as a measure of bonding was calculated between substitutional indium and interstitial nitrogen. It equals 0.15 in the absence of boron. With boron present in a substitutional site, the overlap population increases to 0.26. That is, the bonding between indium and nitrogen is enhanced by the presence of boron. Experimentally, this prediction appears to be supported when comparison is made between sets of as-implanted (In+N) and (In+B+N) and annealed (In+N) and ($In+B+N$). SIMS measurements are displayed in Figure 4. Note that almost all diffusion of the indium is suppressed in the ($In+B+N$) sample while there is noticeable diffusion both towards the surface as well as into the substrate for the ($In+N$) sample.

VI. Conclusion

The insights gained on the atomistic level and the close correlation with experimental results permits creation of retrograde channels with desired slopes and threshold voltage characteristics. Since device geometries are being aggressively shrunk, regions where several dopant species and heterostructures are present will play even greater roles in determining critical aspects of device behavior. Insight into the interactions as well as understanding diffusion control options will be very attractive. Finally, though interstitials and vacancies in continuum modeling are used to describe and determine complex dopant diffusion behavior, the quantum chemical picture suggests that there are additional factors to be considered [7].

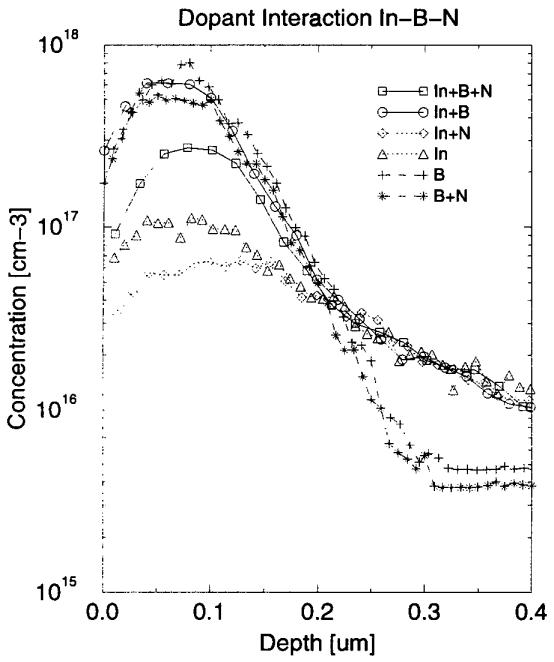

Fig. 3. Spreading resistance profiles for all the combinations of boron, indium and nitrogen presented in Table I.

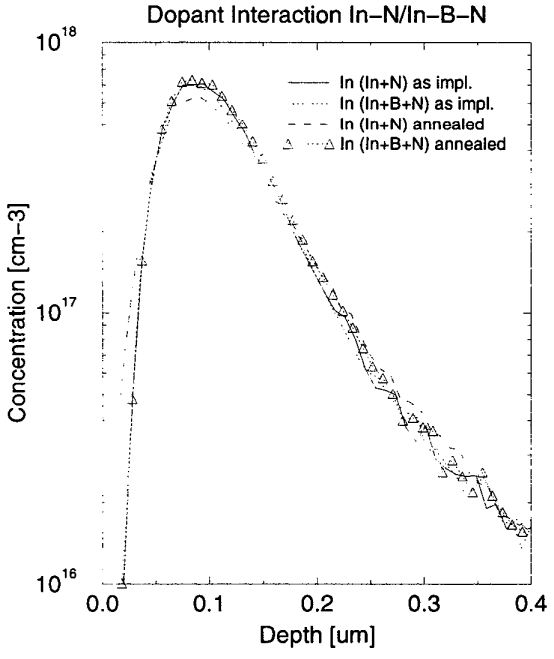

Fig. 4. SIMS profiles of indium. The as-implanted In+N, In+B+N and annealed In+B+N coincide.

ACKNOWLEDGMENT

The authors would like to thank James Kimball for his diligence in coordinating and executing the experimental phase.

REFERENCES

[1] E. Clementi and D. L. Raimondi, J. Chem. Phys., Vol. 38, pp. 2686–2689 (1963).

[2] E. Clementi, D. L. Raimondi, and W. P. Reinhardt, J. Chem. Phys., Vol. 47, pp. 1300–1307 (1967).

[3] R. S. Mulliken, J. Chem. Phys., Vol. 23, pp. 1833–1840 (1955).

[4] R. S. Mulliken, J. Chem. Phys., Vol. 23, pp. 1841–1846 (1955).

[5] S. Aronowitz, J. Appl. Phys., Vol. 61, pp. 2495–2500 (1987).

[6] S. Aronowitz, L. Coyne, J. Lawless, and J. Rishpon, Inorg. Chem., Vol. 21, pp. 3589–3593 (1982).

[7] S. Aronowitz, J. Appl. Phys., Vol. 70, pp. 6815–6820 (1991).